JOURNAL OF MATERIALS SCIENCE 14 (1979) 2679–2687

Compliances and failure modes of oriented chain-extended polyethylene

G. E. ATTENBURROW, D. C. BASSETT
J. J. Thomson Laboratory, University of Reading, UK

The quantitative dependence of Young's modulus and fracture behaviour on the angle between the tensile axis and the orientation direction has been determined for oriented polyethylene with lamellae of chain-extended dimensions. The form of the modulus dependence was similar to that for the majority of oriented polymers which have been studied, but the fracture behaviour was atypical, ductility only being obtained when the test axis was parallel to the orientation direction, with brittle fracture occurring in all other directions for all except very high molecular mass materials.

The behaviour of this material in compression along *c* has also been studied; in this case kink bands and *c*-axis cleavage were observed. It is shown that kink band formation may be explained solely by uniform *c* axis shear deformation of the lamellar crystals.

1. Introduction

Semi-crystalline polymers prepared by melt crystallization at atmospheric pressure usually have a complicated hierarchy of microstructures and an extremely small basic morphological unit (the folded-chain lamella). Systematic study of the dependence of mechanical properties on any one unit of microstructure for polymers in such form has not yet been possible.

Treatment at high pressures simplifies the problem by producing a microstructure of crystalline lamellae, 0.1 to $\sim 10\,\mu m$ thick, readily observed and quantitatively analysed by a variety of techniques [1,2] and which can be prepared in a form virtually free from any complicated higher level spherulitic texture. A further simplification of structure is achieved in the case of oriented chain-extended polyethylene [3], prepared by high pressure annealing cold-drawn polyethylene in the hexagonal phase [4]. Thus oriented chain-extended polyethylene presents us with an especially favourable situation for investigating the dependence of mechanical behaviour on lamellar microstructure in semi-crystalline polymers.

In an earlier work Bassett and Carder [5] reported the variation of simple mechanical properties, namely modulus along the *c*-axis and ductility for oriented polyethylene as the lamellar thickness increased from about 20 to 200 nm. In the present publication the mechanical behaviour of oriented chain-extended polyethylene is explored in more detail. The dependence of the tensile modulus and fracture behaviour on the angle between the test direction and orientation axis and also microscopic aspects of the deformation in compression have been measured.

2. Experimental method

2.1. Materials

The polyethylene used was "Rigidex 9"* from which low molecular mass material to about 10^4 had been removed by extraction with boiling amyl acetate. Gel permeation chromatographic analysis of a typical residual material gave a mass average molecular mass ($\bar{M}_m$) of 1.67×10^5 and a number average molecular mass ($\bar{M}_n$) of 3.79×10^4 with a dispersity of 4.4.

2.2. Preparation of oriented chain-extended specimens

Sheets, 15 cm × 17 cm × 0.09 cm, of this polyethylene were moulded at $154 \pm 2^\circ$ C under a load of 10 tons for 1 min and then quenched in cold water. A large dumb-bell shaped specimen cut

*B.P. Chemicals Ltd.

0022/2461/79/112679–09 $02.90/0

TABLE I Changes in molecular orientation and specimen dimensions on annealing

Angle between tensile axis and molecular orientation axis		Gauge length (cm) after annealing (originally 2.0 cm)	Gauge width (mm) after annealing (originally 1.45 mm)	Change in thickness
Before annealing	After annealing			
0°	0°	1.6	1.5	All specimens showed a small increase of ~ 10%
15°	20°	1.7	1.5	
30°	34°	1.7	1.4	
38°	45°	1.75	1.3	
55°	63°	2.0	1.2	
90°	90°	2.2	1.1	

from the mould was drawn on an Instron tensile testing machine at room temperature and head speed of 0.2 cm min^{-1} to a natural draw ratio of 6.7 ± 0.3. The drawn region had a width of 4.5 cm and a thickness of 0.3 mm. Dumb-bell shaped tensile specimens with a gauge length of 2.0 cm and width of 1.45 mm were cut at various angles (θ) to the draw direction and subjected to high pressure annealing treatments to increase the lamellar thickness. Following this, the *c*-axis made an increased angle with the gauge length (except for $\theta = 0°$ and 90°), and certain dimensions changed as listed in Table I. High pressure annealing was carried out in a piston and cylinder apparatus [3] at a pressure of 5.3(5) kbar using silicone oil as a pressure transmitting fluid. The annealing temperature of 244 ± 1° C (cf. [3, 6]) was reached in about 2 h and held for 15 min. Specimens were then cooled to ambient temperature over several hours before the pressure was released and residual silicone oil washed off. While in the high pressure chamber specimens were lightly held between thin metal sheets with spacers placed close to and parallel with the gauge length; the sheets inhibited any tendency for specimens to buckle and the spacers ensured that the gauge length remained straight. Specimens annealed without these precautions sometimes became distorted. The specimens were, however, free to expand or contract.

Small cubes (~2 mm side) for compression testing were cut from drawn polyethylene (a similar sample to that described in Section 2.1); the cube sides were parallel and perpendicular to the drawn direction. Such cubes were annealed at high pressure as described above. As was the case with the $\theta = 0°$ dumb-bell specimens, these cubes showed a reduction in length of 20% along the *c*-axis after annealing.

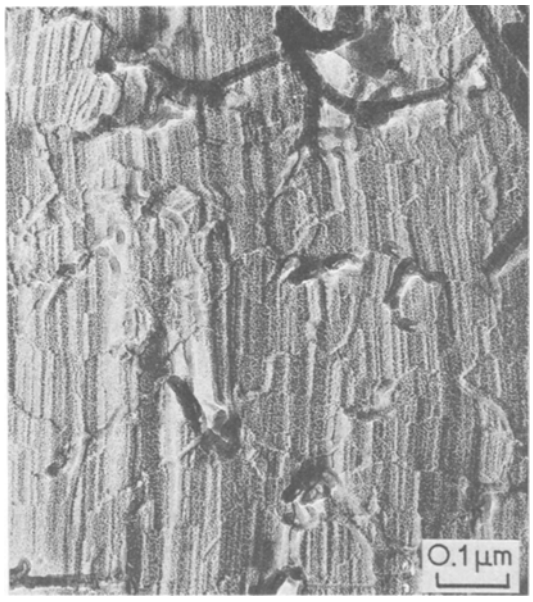

Figure 1 Electron micrograph of a fracture surface of undeformed oriented chain-extended polyethylene.

2.3. Specimen characterization

Table I lists changes suffered by the tensile test specimens following high pressure treatment. There was, however, very little loss of molecular orientation. The product had a density of 0.995 ± 0.0005 g cm^{-3} at 23.0° C and a peak differential thermal melting temperature (measured at 4 K min^{-1}) of 137.9° C. Lamellar thickness was measured in two ways; firstly by direct measurement on fracture surface replicas such as Fig. 1 and appropriate sampling techniques [3]. The lamellae appear as groupings of fine parallel fracture-induced striations lying paralled to the *c*-axis [4]; the lamellar thickness

was measured along this direction and gave a number average value $\bar{L}_n$ of 97 nm and a mass average $\bar{L}_m$ of 112 nm. The second technique measured the molecular lengths left after treating specimens in fuming nitric acid at 60° C for 3 days. Values obtained by Gel Permeation Chromatography gave $\bar{L}_n = 111$ nm and $\bar{L}_m = 158$ nm. This agreement between different averages of the two measuring techniques is a feature which has been recognized [7] and discussed [8] elsewhere.

2.4. Mechanical testing

Specimens were tested at room temperature, in tension and compression, on an Instron Model 1115 testing machine. The dumb-bell shaped specimens were tested in tension at a cross-head speed of 0.05 cm min^{-1} until fracture occurred. At least three specimens were tested for each angle (θ) considered; fracture usually occurred within the gauge length.

The cubes were tested in compression with the axis of compression along the draw direction and at a cross-head speed of 0.005 cm min^{-1} giving a similar strain rate to the samples tested in tension). When the samples had been subjected to a compressive strain of ~15% they were removed and examined in both the optical and transmission electron microscopes. Structure was observed in the optical microscope either by examining the compressed cubes directly or by examining acetate replicas of fracture surfaces which were parallel to both the *c*-axis and one of the cube faces. Specimens for transmission electron microscopy were two-stage carbon replicas of the same fracture surfaces.

3. Results

3.1. Initial modulus

Fig. 2 shows typical engineering stress (load/original cross-sectional area) versus strain curves. Specimens tested along the direction of orientation showed a yield point, with no load drop, followed by drawing to between 4% and 13% strain before final fracture. Specimens of all other values of θ showed brittle fracture at low strains (~1%).

Measurement of the initial Young's modulus was made from the curves, a small correction being made for machine compliance. The variation of modulus E_θ with θ (the value after annealing) is shown in Fig. 3 and it can be seen that the material is rather anisotropic in this respect with $E_0 = 6.7$ GPa, $E_{45} = 2.4$ GPa, $E_{90} = 2.5$ GPa. As θ increases from zero the modulus falls sharply but by 30° the rate of fall has slowed and from 45° onwards the modulus is relatively invariant. The solid curve in Fig. 3 was obtained by inserting the experimentally determined values of E_0, E_{45} and E_{90} into the equation

$$\frac{1}{E_\theta} = s_{11} \sin^4\theta + (2s_{13} + s_{44}) \sin^2\theta \cos^2\theta + s_{33} \cos^4\theta$$

where s_{11} etc. are compliance components [9]. There is good agreement with the other points, demonstrating the applicability of classical elasticity theory to this material. Experimental values for the compliances are

$$s_{33} = \frac{1}{E_0} = 0.15 \text{ GPa}^{-1}$$

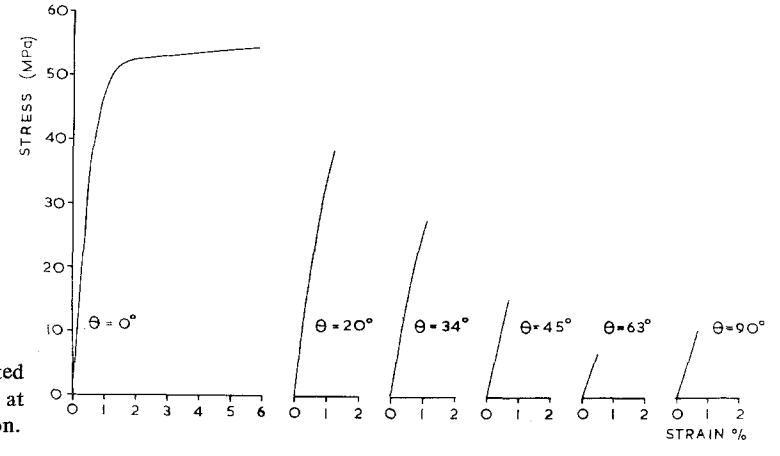

Figure 2 Stress–strain curves for oriented chain-extended polyethylene tested at various angles to the orientation direction.

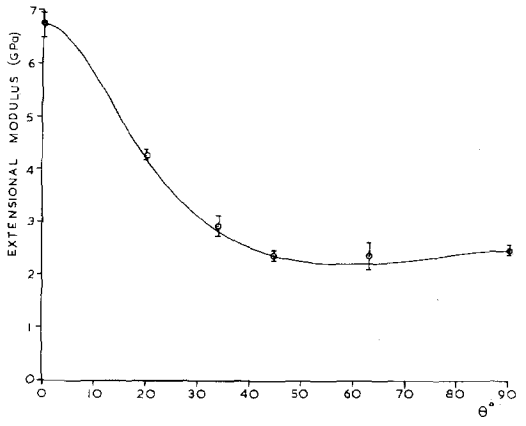

Figure 3 Dependence of extensional modulus of oriented chain-extended polyethylene on the angle θ between tensile test direction and orientation axis.

$$s_{11} = \frac{1}{E_{90}} = 0.40\,\text{GPa}^{-1}$$

and

$$(2s_{13} + s_{44}) = \frac{4}{E_{45}} - (s_{11} + s_{33}) = 1.1\,\text{GPa}^{-1}.$$

An estimate of the values of the other compliances may be made on the assumption, reasonable at small strains, that the deformation occurs at constant volume. We then have [9]

$$s_{11} + s_{12} + s_{13} = 0$$

and

$$s_{33} + 2s_{13} = 0$$

leading to the numerical values of

$$s_{44} = 1.37\,\text{GPa}^{-1}$$

$$s_{12} = -0.33\,\text{GPa}^{-1}$$

and

$$s_{13} = -0.07\,\text{GPa}^{-1}.$$

Following recent work of Arridge and Folkes [10] one has to consider the effect clamping the specimen may have on the values of moduli measured. It has been shown that for highly anisotropic samples (draw ratio ~30) aspect ratios approaching 100 may be required to produce the correct value. Our specimens are considerably less anisotropic than this and one does not, therefore, anticipate serious inaccuracies arising in this way. As an experimental check measurements of the velocity of transmitted sound (cf. [11]) were made on certain of the specimens leading to the values

$$s_{33} = 0.035\,\text{GPa}^{-1}$$

and

$$s_{11} = 0.12\,\text{GPa}^{-1}$$

These values are both lower, by a factor of about four, than those measured in tensile tests, doubtless due to the high frequencies used in the ultrasonic determination. It is noteworthy, however, that the ratio s_{33}/s_{11} is 3.5 acoustically and 2.7 mechanically. This reasonable agreement would not have been expected if there were serious end-effects in the tensile tests as these would have been much more pronounced for E_0 than for E_{90} because of sample anisotropy. This is taken as evidence that the relatively small aspect ratios we have had to use have produced no major systematic error in the data.

3.2. Yield and fracture behaviour in tension

Ductile fracture only occurred in tension parallel to the orientation axis. In this case there was a yield point at ~1% strain followed by cold draw with no observable neck formation until fracture at 4 to 13% strain (see Fig. 2). Such specimens, initially translucent, displayed whitening as drawing progressed.

The variation of nominal fracture stress (σ_θ = fracture load/original cross-sectional area) with θ is shown in Fig. 4. As can be seen σ falls from ~50 MPa at $\theta = 0°$ to a shallow minimum of ~8 MPa at $\theta = 63°$, and then rises slightly to ~11 MPa at $\theta \sim = 90°$. In specimens which showed ductile fracture the fracture surfaces were perpendicular to the orientation axis for two of the specimens and inclined at 12° for the third. In the case of specimens showing brittle fracture, the fracture surfaces were parallel to the orientation axis for $\theta = 90°$ and 63° but for $\theta = 20°$, 34° and

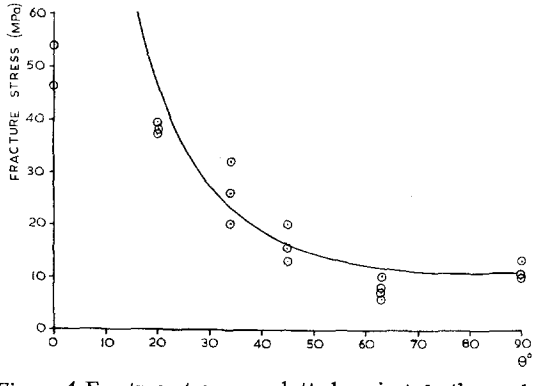

Figure 4 Fracture stress σ_θ plotted against θ, the angle between the tensile test direction and orientation axis. The solid curve is given by

$$\sigma_\theta = \frac{58.4}{(\sin 2\theta + 5.22 \sin^2\theta)}.$$

45° the angle between fracture surface and tensile test direction was some 10° greater than θ. An equation of the form

$$\sigma_\theta = \frac{A}{(\sin 2\theta + B \sin^2 \theta)}$$

best fits the values of θ for $\theta > 0$.

The solid curve in Fig. 4 was obtained from this equation (which is of the same form as that which would be obtained if a Coulomb criterion of fracture were used) using the experimental values of σ_{45} and σ_{90} which give:

$$A = 58\,\text{MPa}$$

$$B = 5.2.$$

3.3. Behaviour in compression

Typical stress–strain behaviour in compression down the c-axis is illustrated in Fig. 5. A siginificant feature of this curve is the appearance of several instantaneous load drops. A sample which had been compressed in this way is shown in Fig. 6a. The orientation (c) axis is vertical and parallel to the axis of compression. Dark bands (arrowed "a") of various widths (~5 to 30 μm) can be seen forming an angle (ϕ) with the orientation axis. Measurements from several micrographs gave values of ϕ between 53° and 63°. Fig. 6b shows the optical appearance of an acetate replica of a fracture surface. The orientation (c) axis is delineated by a surface texture of striations and within the band the c-axis is very much tilted away from its original direction. Measurements from several optical micrographs of the cubes themselves and replicas showed that this c-axis rotation varied between 54° and 74°. Similar bands to these have been observed in both polymers [12] and metals [13] and are referred to as kink bands. The black line (arrowed "b" in Fig. 6a) is identified as cleavage paralled to c due to buckling of the sample during compression; it can be seen that this cleavage follows local variations of c-axis direction within the kink bands (arrowed "c" in Fig. 6a).

Examination of fracture surface replicas in the transmission electron microscope allows the observation of finer details. Fig. 7a shows that within the kink band lamellar boundaries are invariably inclined obliquely to the local c-axis in contrast to the undeformed situation of Fig. 1 (i.e. the lamellae have become sheared). The angle α between boundary and c-axis is 40°. Fig. 7b shows the appearance at the kink band boundary which runs from top left to lower right, the lower portion of the micrograph being within the kink band. Fig. 8 illustrates the geometry of the kink bands. The values of the angles shown were taken from the kink band shown in Fig. 6b, which was examined by transmission electron microscopy.

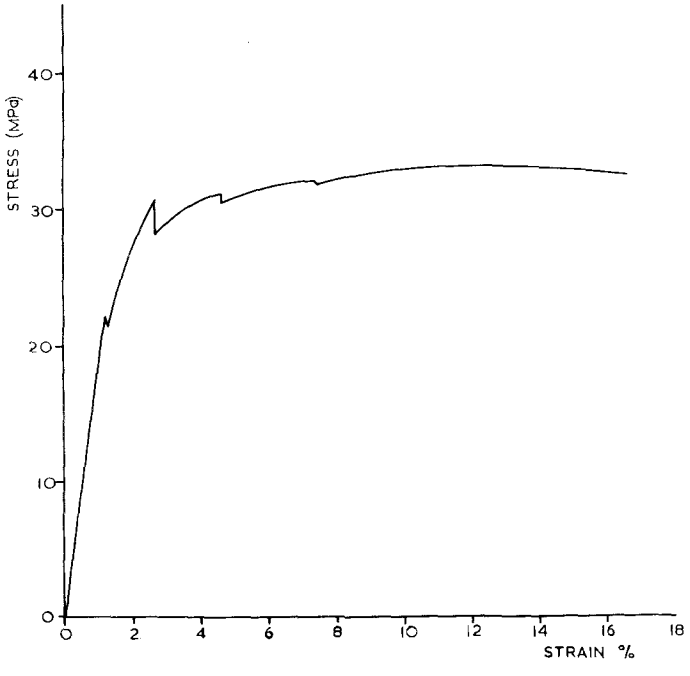

Figure 5 Stress–strain curve for oriented chain-extended polyethylene tested in compression along the orientation axis.

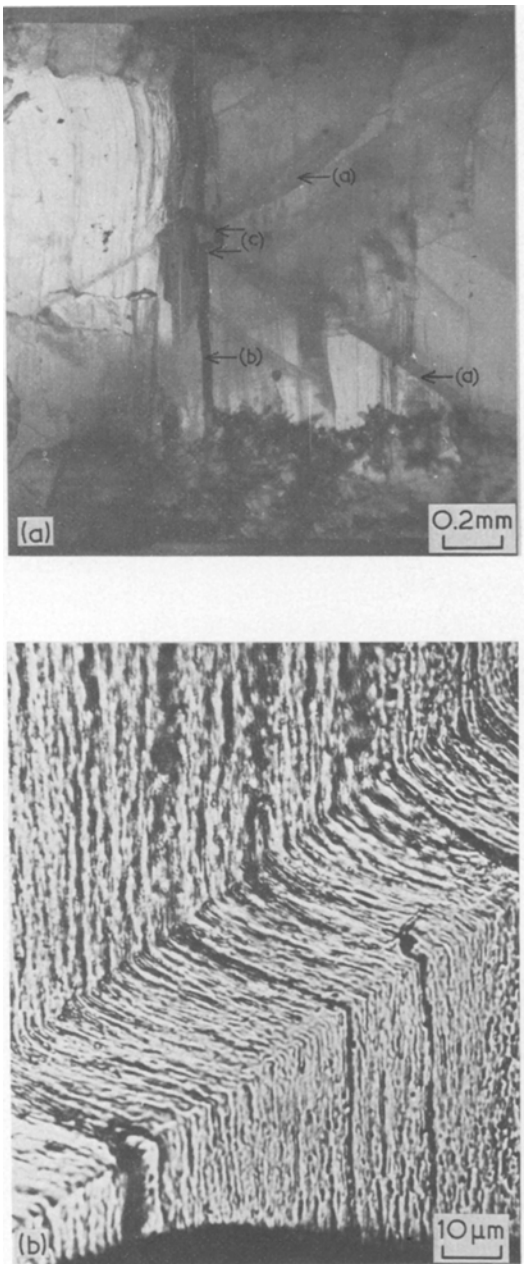

Figure 6 The appearance of kink bands in a sample of oriented chain-extended polyethylene which had been subjected to ~15% compressive strain. (a) As viewed directly in the optical microscope; (b) an acetate replica of a fracture surface as viewed in the optical microscope.

Finally, electron microscopy revealed some finer scale kink bands whose dimensions were of the same order as the lamellar thickness. These are shown in Fig. 9.

4. Discussion

4.1. Anisotropy and elastic constants

The main feature of the mechanical anisotropy of pressure-annealed drawn polyethylene is the similarity to that of the original cold-drawn fibre. Reference to Table II shows that both these materials are broadly similar to drawn polypropylene but not to low-density polyethylene and PTFE for which the compliance s_{44} is exceptionally large. Although numerical values for different authors are probably not strictly comparable it is clear, nevertheless, that the large increases in crystal thickness and lateral size (plus the associated variables of density and melting point) have had small mechanical consequences. There are small changes, noted by Bassett and Carder [5], as the additional stiffening produced by cold-drawing relaxes at an early stage of increasing lamellar thickness but the conclusion previously reached on morphological grounds [3], that annealing in the high-pressure disordered hexagonal phase produces, to a first approximation, no major change in the nature of interlamellar regions, is now supported also by these mechanical data on anisotropy. The decrease in compliances s_{33} and s_{11} with annealing temperature is a consequence of a declining proportion of soft interlamellar regions between ever thicker crystals. A simple series model of infinitely wide lamellae sandwiched between interlamellar disordered zones corresponding to the observed morphology has been shown to fit data for s_{33} [5]. There have, however, to be major changes in the nature of the disordered region and their coupling to crystals for the stiffness of real samples to approach the theoretical value for the polyethylene crystal. Annealing and crystallization treatments in either orthorhombic or hexagonal phases do not do this of themselves. It is intuitively reasonable, however, that severe deformation (very high draw ratios) could effect such a change and this appears to be the physical basis of the very stiff drawn fibres which have recently been produced [16].

4.2. Fracture in tension

Significant mechanical differences produced by annealing cold-drawn specimens under pressure do appear when yielding under tension is examined. Whereas Keller and Rider [17] observed that cold-drawn linear polyethylene gave no brittle fracture in tension, this was observed following annealing

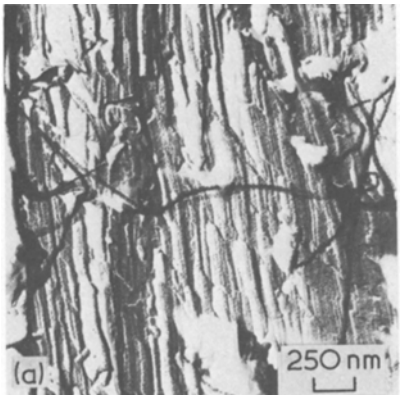

Figure 7 Electron micrographs of two-stage replicas of a kink band in oriented chain-extended polyethylene. (a) Lamellar crystals within the kink band. (b) A kink band boundary.

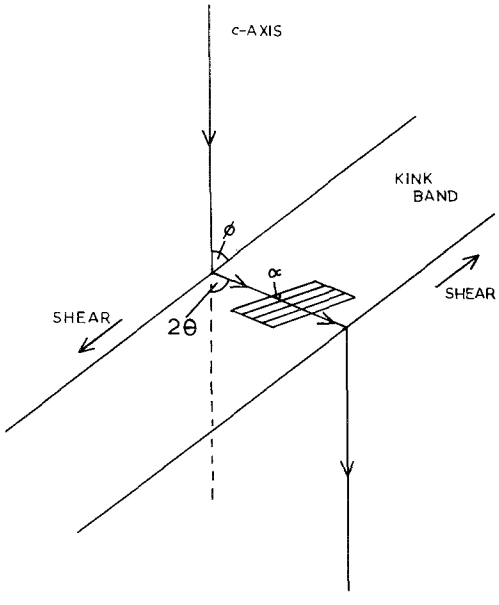

Figure 8 Diagram of the typical geometry of a kink band.

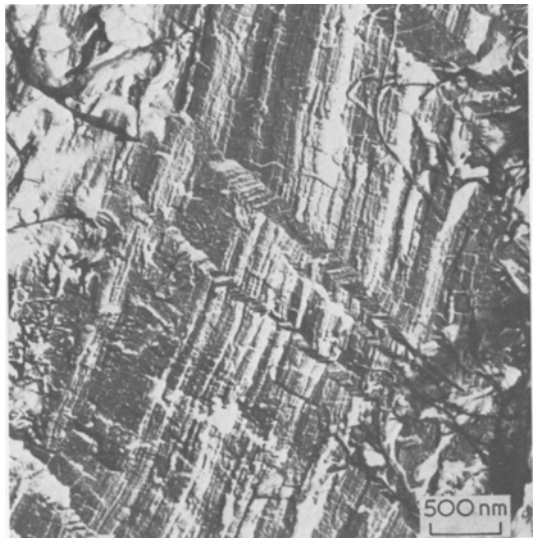

Figure 9 Smaller kink bands of the same order of thickness as lamellar crystals.

TABLE II Elastic constants of oriented polymers

Polymer	Draw ratio	s_{11} (GPa^{-1})	s_{33} (GPa^{-1})	s_{44} (GPa^{-1})	s_{11}/s_{33}
Chain extended oriented linear polyethylene (this work)	5.5	0.40	0.15	1.37	2.7
Drawn linear polyethylene [14]	5.5	1.6	0.4	2.0	4.0
Cold-drawn branched polyethylene [14]	5.5	3.6	1.6	100	2.2
Drawn polypropylene [14]	5.5	1.1	0.3	1.5	3.7
Cold-drawn polytetrafluoroethylene [15]	2.6	2.6	2.4	15	1.1

at atmospheric pressure for θ (the angle between specimen and fibre axis) greater than 75°. The pressure-annealed specimens of this paper fractured brittly for $\theta > 0$ and were ductile only for $\theta = 0$. A specific cause of brittle fracture was identified in earlier work [3] as the segregation and separate lamellar crystallization between the largest (and first-formed) crystals of low molecular weight polymer (< about 10^4 molecular mass). This is now known to result because such short molecules do not enter the hexagonal phase on annealing at 5 kbar [1]. They would, therefore, be expected to have melted from the orthorhombic phase when the annealing temperature was reached and to occupy available interstices between the thick crystals of the hexagonal phase where they would recrystallize directly as orthorhombic lamellae on cooling. Fractionation and physical separation in this manner is normal during crystallization treatments at high pressure [1, 18] and also occurs, at least for high crystallization temperatures (~ 130° C), at 1 bar [19].

With removal of such short molecules from Rigidex 9 polyethylene the annealed oriented polymer becomes ductile for tension along the orientation axis only; unoriented polymer of this molecular mass is always brittle. Brittleness does, however, disappear for all θ when the high molecular mass ($M_m > 2 \times 10^6$) Hifax polyethylene is used [20]. There appears to be a simple explanation. It is that only when molecular length is a reasonably large (> 10) multiple of crystal thickness are there sufficient intermolecular tie molecules to blunt cracks. Furthermore, there is considerable evidence of fractionation and segregation within polydisperse polyethylenes following high pressure crystallization; molecules of similar lengths tend to solidify together [1, 18]. In consequence there are likely to be potentially brittle lamellae present following high pressure crystallization or annealing of polyethylene unless molecules shorter than about ten times the crystal thickness, say 5×10^5 in mass, are absent. This is entirely in accord with our experience.

4.3. Behaviour in compression

The introduction of kink bands for compression down the *c*-axis has parallels with the behaviour of hexagonal metals [13]. Similar features are also reasonably common in the thickest lamellae produced by crystallizing polyethylene at 5 kbar. Then they occur within individual crystals and appear to be a consequence of deformation twinning with {0 1 1} as twin plane. This is inferred from the figure of 62° for the mean angle between the plane and the *c*-axis for 200 such features, on the assumption that fracture tends to expose {2 0 0} planes preferentially [18, 19]. In the present example samples only have fibre symmetry around *c*, making their crystallography less well-defined. There has, however, been consideration of how such kinking might be caused when they have been produced in polyethylene in other ways [21, 22]. The major conclusion of others has been that the common deformation mode of uniform shear parallel to *c* is insufficient to account for the observation, but that an additional mechanism such as intermicrofibrillar or interlammellar slip must also be invoked. This does not, however, appear to hold for the observations reported here which are close to what would be predicted for a mechanism of uniform shear parallel to *c* alone. Referring to Fig. 8, the angle ϕ between a kink plane and the *c*-axis and the angle 2θ by which the *c*-axis rotates are both easily measured while the angle α between the lamellar surfaces and *c* within a band can be directly observed in fracture surfaces. For the kink band in Fig. 7, $\phi = 53°$,

$2\theta = 67°$ and $\alpha = 40°$; these are close to the values predicted in Fig. 11 of [21]. More specifically one expects that

$$\theta + \phi = \pi/2,$$

i.e. that the kink plane should bisect the angle between the two c-axis directions; this is usually nearly so but may not hold exactly. It is then easy to show that

$$\tan \alpha = \tfrac{1}{2} \tan \phi.$$

Taking $2\theta = 67°$ would give accordingly $\phi = 56.5°$ and $\alpha = 37°$, in fair agreement with observed values. It seems reasonable to conclude, therefore, that uniform shear parallel to c is more important for the pressure-annealed samples than for the different specimens examined by others [21,22]. This is a similar trend of behaviour to that observed for failure in tension and is likely to have a similar origin in changes in the interlamellar regions which make them more prone to shear deformation.

5. Conclusions

(1) The anisotropy of Young's modulus for pressure-annealed polyethylene fibres is similar to that for the original unannealed cold-drawn specimens. This implies that the interlamellar regions are mechanically similar in both cases. This confirms previous results which showed that annealing and crystallization treatments lead to wide and soft lamellar interfaces with only modest increases in chain axis stiffness, as would be expected from a series composite model. To obtain exceptional increases in axial stiffness it is necessary to find some means of overcoming this weakness, for example by severe disruption on stretching to very high draw ratios [16].

(2) Brittle fracture is the usual means of failure under tension. Two causes of this have been identified. (i) Molecules less than about 10^4 in mass crystallize separately between the characteristic large lamellae and are the site of fracture [5]. (ii) The persistence of brittleness for tension along all directions except c in polymer without such short molecules is associated with a low ratio of molecular length to crystal thickness. This is believed to make the interlamellar regions less able to blunt cracks and resist other flaws.

(3) In compression down c, yield is discontinuous and occurs by buckling and kinking. The observations on kinking are consistent with its production solely by uniform shear parallel to c.

Acknowledgements

The authors wish to express their gratitude to Mr K. Thomas and Dr M. J. Richardson of the National Physical Laboratory for allowing the acoustical measurements of compliance.

References

1. D. C. BASSETT, *Polymer* **17** (1976) 460.
2. *Idem, High. Temp. High. Press.* **9** (1977) 553.
3. D. C. BASSETT and D. R. CARDER, *Phil. Mag.* **28** (1973) 513.
4. D. C. BASSETT, S. BLOCK and G. J. PIERMARINI, *J. Appl. Phys.* **45** (1974) 4146.
5. D. C. BASSETT and D. R. CARDER, *Phil. Mag.* **28** (1973) 535.
6. D. C. BASSETT, B. A. KHALIFA and R. H. OLLEY, *Polymer* **17** (1976) 284.
7. *Idem, J. Polymer Sci. Polymer Phys. Ed.* **15** (1977) 995.
8. R. H. OLLEY and D. C. BASSETT, *ibid.* **15** (1977) 1011.
9. J. F. NYE, "Physical Properties of Crystals" (Oxford, 1957) Ch. 8.
10. R. G. C. ARRIDGE and M. J. FOLKES, *Polymer* **17** (1976) 495.
11. K. THOMAS and D. E. MEYER, *Plast. & Rubber Mater. & Appl.* **1** (1976) 136.
12. R. G. ROBERTSON, *J. Polymer Sci. A-2* **7** (1969) 1315.
13. R. W. K. HONEYCOMBE, "The Plastic Deformation of Metals" (Arnold, London, 1968) Ch. 8.
14. D. W. HADLEY, P. R. PINNOCK and I. M. WARD, *J. Mater. Sci.* **4** (1969) 152.
15. R. DAVITT, Ph.D. Thesis, University of Reading (1973).
16. G. CAPACCIO and I. M. WARD, *Polymer* **15** (1974) 233.
17. A. KELLER and J. G. RIDER, *J. Mater. Sci.* **1** (1966) 389.
18. D. C. BASSETT and A. M. HODGE, (to be published).
19. *Idem, Proc. Roy. Soc. A* **359** (1978) 121.
20. G. E. ATTENBURROW and D. C. BASSETT, *J. Mater. Sci.* **12** (1977) 192.
21. K. SHIGEMATSU, K. IMADA and M. TAKAYANAGI, *J. Polymer Sci. Polymer Phys. Ed.* **13** (1975) 73.
22. A. G. KILBECK and D. R. UHLMANN, *J. Polymer Sci. Polymer Phys. Ed.* **14** (1976) 1257.

Received 27 February and accepted 12 March 1979.